Vol.4, No.3, Page 1825- 1830, 2026 https://doi.org/10.59628/jast.v4i3.2488 ISSN 2958-9568 JAST

SUN PUBLISHER

مجلة جامعة صنعاء للعلوم التطبيقية والتكنولوجيا

Sana'a University Journal of Applied Sciences and Technology

https://journals.su.edu.ye/index.php/jast/

Green Synthesis and Characterization of ZnO and MgO Nanoparticles Using Chamomile Extract

Ali Hashim Mohammed [1], Ali Maajal Ali[2], Mohaimen Baseem Awf[1], Rafaa Abd Alkareem Abdulwahid[1], Laith Salih Mohammed[1]* and Ghassan Adnan Naeem[1]

[1]**Department of Medical Physics, Faculty of Applied Sciences and Hit, University of Anbar, Anbar, 31007, Iraq,**
[2]**Department of Environment, Faculty of Applied Sciences, Hit, University of Anbar, Anbar, 31007, Iraq.**

*Corresponding author: laith2011alhiti@uoanbar.edu.iq

Abstract

Green synthesis offers an environmentally benign approach for producing functional metal oxide nanomaterials. In this study, chamomile extract was employed as a natural reducing and stabilizing agent to synthesize ZnO and MgO nanoparticles under identical reaction conditions. The nanoparticles were prepared at 30 °C for 30 min under neutral pH, followed by heat treatment at 400 °C for five hours to remove residual moisture and promote crystallization. Structural and morphological characteristics were examined using X-ray diffraction (XRD), UV–visible spectroscopy and scanning electron microscopy (SEM). The UV–Vis spectra exhibited characteristic absorption peaks at 369 nm for ZnO and 265 nm for MgO. XRD analysis confirmed the formation of hexagonal wurtzite ZnO and face-centered cubic MgO phases, with calculated crystallite sizes of 8.35 nm and 11.58 nm, respectively. SEM images revealed predominantly spherical ZnO nanoparticles forming agglomerated secondary structures (55–70 nm) and spherical MgO nanoparticles with primary sizes ranging from 60–75 nm. The results demonstrate that chamomile extract serves as an effective biotemplate for controlling the nucleation and growth of ZnO and MgO nanoparticles, leading to well-defined structural and morphological features. This study highlights the potential of plant-mediated synthesis as a sustainable route for producing stable nanomaterials suitable for biomedical and environmental applications, reinforcing the role of green chemistry in advancing eco-friendly nanotechnology.

Article Info

Keywords:
Green synthesis, Nanoparticles, Characterization, Zinc Oxide (ZnO), Magnesium Oxide (MgO), X-ray diffraction (XRD), Scanning electron microscopy (SEM).

Article History:
Received: 7-November-2025,
Revised: 20-January-2026,
Accepted: 29-January-2026,
Published: 28 March 2026.

1. INTRODUCTION

Nanomaterials based on metal oxide semiconductors have great potential for a wide range of industrial applications [1]. Among such, zinc oxide (ZnO) and magnesium oxide(MgO) possess unique physical and chemical properties. High efficiency, stability, low cost, and non-toxic nature make them useful for catalysis, optoelectronic devices, and chemical/biological sensors-nanotechnology [2]. Nano-composites of ZnO, ZnO-MgO, and ZnO exhibit enhanced optical properties, including a wider band gap owing to the electronic interaction between ZnO and MgO. Solid-state reaction, electrochemical method, hydrothermal synthesis by sonic chemical process, and sol-gel process thermal evaporation deposition have been reported to fabricate nanostructures of MgO [3]. This study presents a simple, economical, and green one-step co-precipitation method for the synthesis of ZnO, ZnO–MgO nanocomposites (NC-1, NC-2, and NC-3), and MgO nanocomposites using chamomile. The formed nanomaterials were fully characterized using spectroscopy and microscopy. Although a variety of plant extracts have been utilized in the green synthesis of metal oxide nanoparticles, most existing studies focus on the synthesis of a single oxide material, making it difficult to compare how different metal precursors respond to the same phytochemical environment. Furthermore, reports

involving chamomile extract primarily investigate its reducing capability for one type of nanoparticle without examining its simultaneous effect on multiple metal oxides under controlled and identical conditions. Therefore, there remains a lack of systematic studies that use the same plant-mediated route to directly compare the nucleation behavior, crystallinity, and morphological evolution of different metal oxide nanoparticles. This study aims to address this gap by employing chamomile extract as a unified biotemplate to synthesize ZnO and MgO nanoparticles under the same experimental parameters, thereby enabling a clearer understanding of how a single phytochemical profile governs their formation.

In this study, we developed a green synthesis method for ZnO and MgO nanoparticles using chamomile extract as a natural reducing and stabilizing agent under identical reaction conditions. This study specifically focused on synthesizing these nanoparticles and characterizing their structural and optical properties, as well as investigating their morphology and particle size distribution via SEM analysis. Furthermore, the effects of chamomile extract on the nucleation, growth, and crystallinity of ZnO and MgO nanoparticles were systematically compared. Finally, we evaluated the potential of plant-mediated synthesis as a sustainable and eco-friendly route for producing stable metal oxide nanomaterials with potential applications in the biomedical and environmental fields. This paragraph clearly defines the scope and direction of the study and highlights its novelty in the field of green nanomaterial synthesis.

Although numerous studies have reported the green synthesis of metal oxide nanoparticles using various plant extracts, limited attention has been paid to a direct comparative synthesis of ZnO and MgO nanoparticles prepared under identical biological and reaction conditions using the same plant source. Most previous studies have focused on synthesizing a single metal oxide, making it difficult to evaluate the influence of plant-mediated phytochemicals on different metal precursors. In the present work, chamomile extract was used as a unified biotemplate to simultaneously synthesize ZnO and MgO nanoparticles under controlled and comparable conditions, thereby enabling a systematic assessment of how a single phytochemical profile governs nucleation, growth, and final morphology in two distinct metal oxide systems. This comparative green synthesis approach, supported by structural and morphological correlations, distinguishes the novelty of this study and provides insights that have not been previously discussed in the literature.

2. PREPARATION OF THE PLANT-EXTRACT

Chamomile leaves were collected from a farm in the Khazraj village, affiliated with the Hit district, west of the Anbar Governorate, Iraq. The leaves were washed, dried, and ground to obtain a powder. Next, 5 g of the plant powder was placed in 100 mL of deionized distilled water and boiled for half an hour; the solution was then cooled and separated by centrifugation at 1000 rpm [4]. Thereafter, the chamomile extract was placed in a 100 mL flask, as shown in Figure 1, and stored at 4 ℃ until use. and stored at a temperature of 4 ℃ until the plant extract was used [5].

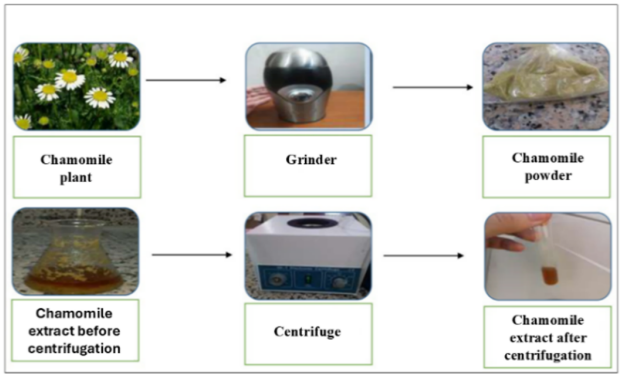

Figure 1. Flow chart showing the steps for preparing a herbal extract from chamomile.

3. PREPARATION OF ZINC OXIDE NANOPARTICLES

First, 0.12 M (2.3 g) of Zn $(NO_3)_2$ $6H_2O$ was added to 75 mL of deionized distilled water. Then The mixture was placed in a magnetic stirrer at a speed of 400 rpm and at a temperature of 70 ℃. After 30 min of adding 20 mL of chamomile extract intermittently to the $Zn(NO_3)_2$ $6H_2O$ solution, a suspension consisting of nanoparticles that were clearly visible to the naked eye was obtained at a pH of 7. The suspension was placed in an air oven at a temperature of 70 to 80 ℃ for 8–10 h to get rid of moisture, after which the powder was obtained. The dried powder was taken and placed in a crucible, and the crucible was placed in a hot oven at a temperature of 50 ℃. then The temperature of the device was automatically raised to 400 ℃ for a period of 35 min. Keep The powder in the hot oven for 5 h at 400℃ to purify the sample from impurities and unwanted particles [6]. The powder was then placed in a desiccator to cool the sample and ground using a mortar to be placed in special tubes, as shown in Figure 2.

4. PREPARATION OF MAGNESIUM OXIDE NANOPARTICLES

First, 0.13 M (2.9 g) of Mg $(NO_3)_2$ $6H_2O$ was placed in 75 mL of deionized distilled water. The mixture was placed on a magnetic stirrer at a speed of 400 rpm and a temperature of 70 ℃. After 30 min of adding 20 mL of

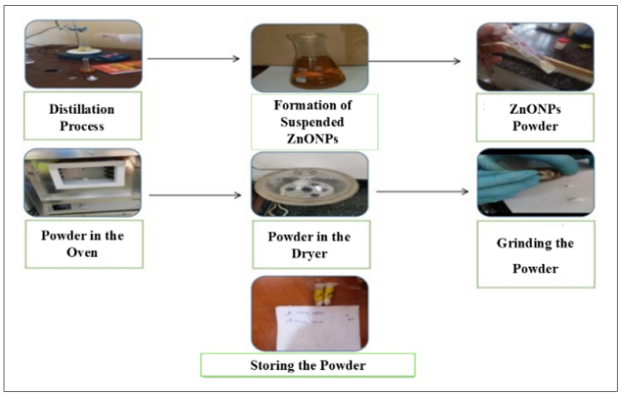

Figure 2. Schematic diagram showing the steps of ZnO nanoparticles.

chamomile extract intermittently to the Mg $(NO_3)_2$ $6H_2O$ solution, a suspension consisting of nanoparticles was obtained at a pH of 7. The suspension was placed in an air oven at a temperature ranging from 70 to 80 ℃ for a period of time ranging from 10 h to get rid of moisture [7]. After obtaining the nano magnesium oxide powder, the powder was taken and placed in a crucible, and the crucible was placed in a hot oven at a temperature of 50 ℃. then The temperature gradually increased to 400 ℃ for a period of 35 min. The sample was kept in the hot oven for 5 h at 400 ℃ to purify the sample, and the powder was placed in a desiccator to cool the sample [8]. Finally, the sample was ground using a mortar and placed in special tubes until use, as shown in Figure 3.

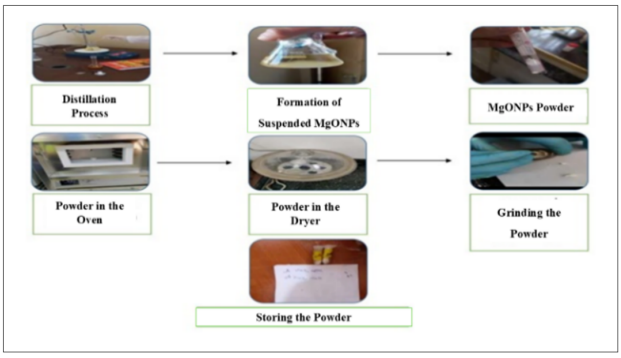

Figure 3. Schematic diagram showing the steps of MgO nanoparticles.

5. RESULTS AND DISCUSSION

5.1. UV-Vis spectroscopy

- **Zinc oxide nanoparticles**
  UV-Vis absorption spectroscopy was used to confirm the formation of nanoparticles [9], as the size of nanoparticles plays an important role in changing the optical properties of materials [10]. Therefore, studying the size of nanoparticles is necessary to explore the properties of materials [11]. The optical absorption spectrum was studied in the range of 200–800 nm using UV-VIS spectroscopy, as shown in Figure 4, where the absorption spectrum of ZnO nanoparticles was observed through the absorption peak that appeared at 369 nm, which is within the range of the standard value for ZnO nanocomposite. The reason for obtaining the absorption spectrum is the compatibility of the collective movement of conduction electrons with the frequency corresponding to (λ_{max}), which results in a resonance state and the absorption of the maximum amount of energy [12].
- **Magnesium oxide nanoparticles**
  As shown in Figure 3, the UV-Vis absorption spectrum of the magnesium oxide nanoparticles indicates an absorption peak at 265 nm, which is consistent with the standard value for MgO nanoparticles. The analysis of UV-Vis absorption depends on measuring the light absorbed due to electronic transitions in MgO nanoparticles. When the metal particles are exposed to light, the oscillating electromagnetic field causes a coherent collective oscillation of the free electrons, and the amplitude of the oscillation reaches a maximum at a certain frequency; therefore, a value is obtained in the absorption spectrum at λ_{max}, where a change in the movement of electrons occurs with time under the same oscillation of the incident electromagnetic wave, and thus absorption occurs, which is considered the identity of the nanoparticles [13].

5.2. Scanning electron microscope SEM

- **Zinc oxide nanoparticles**
  Characterization was performed using scanning electron microscopy (SEM) to analyze the morphology of the ZnO nanoparticles and obtain information about the structure, surface topography, variation in the shape and size of the nanoparticles, and their distribution [14]. The results obtained confirmed the formation or synthesis of ZnO nanoparticles, as shown in Figure 4. The images showed the presence of individual ZnO nanoparticles in addition to a number of clusters resulting from the agglomeration of ZnO nanoparticles. In addition, the particles were mostly spherical in shape, in addition to larger grains with no specific shape for these clusters. From the image, it can also be noted that the size of the ZnO nanoparticles ranged from 70 to 55 nm, which is consistent with previous studies [15].
- **Magnesium oxide nanoparticles**
  SEM reveals information about the shape, size, and distribution of the nanoparticles. Figure 5 shows the synthesized MgO nanoparticles, which are mostly spherical in shape and have a size range of (60–75) nm, which is considered to be in the nano range [16].

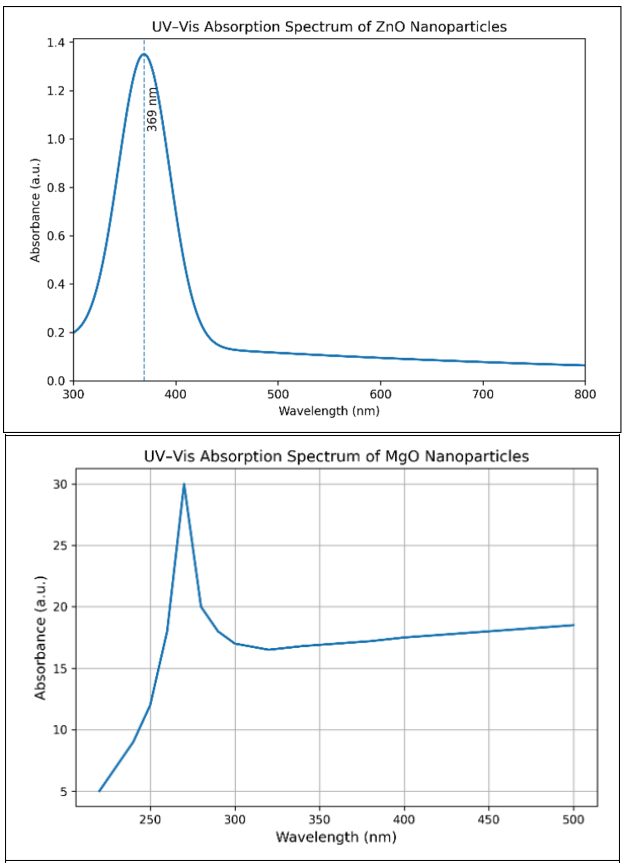

Figure 4. UV-Vis absorbance spectrum, A- ZnO nanoparticles, B- MgO nanoparticles.

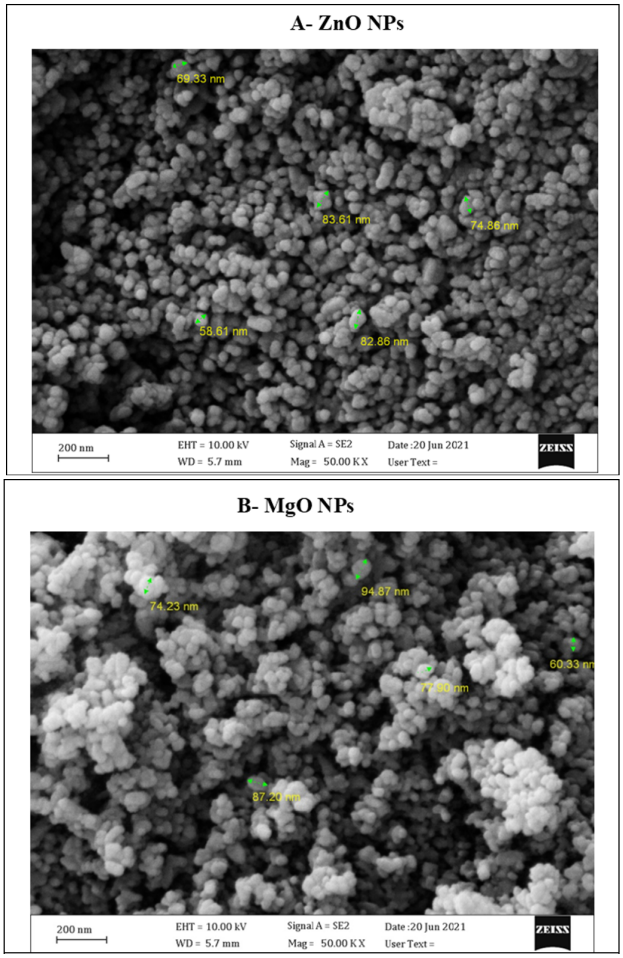

Figure 5. Scanning electron microscope SEM, A-ZnO nanoparticles, B-MgO nanoparticles.

The distribution of the nanoparticles is homogeneous, with some clusters resulting from the agglomeration of MgO nanoparticles, which resulted from the incomplete reaction as well as from the phytochemicals present in the plant extract [17].

5.3. EDX Analysis Technology

- **Zinc oxide nanoparticles**
  The composition of the ZnO sample was determined using EDX. Figure 6 shows the EDX spectra obtained from the green synthesis of ZnO nanoparticles, which are represented by high peaks for both Zn and O with different ratios of 78.06 and 13.07, respectively. In addition, other elements were recorded and attributed to the plant compound used (plant extract) in the synthesis of ZnO NPs [18].
- **Magnesium oxide nanoparticles**
  The MgO nanoparticles were verified by EDX (shown in Figure 6) confirmed that Mg and O were present in high densities, indicating the presence of a MgO compound. The appearance of other atomic elements, such as carbon and potassium, in the spectrum is due to the biomolecules present in the plant extract sample, which acted as reducing and capping agents to produce MgO nanoparticles [19].

5.4. X-ray Diffraction (XRD)

- **Zinc oxide nanoparticles**
  X-ray diffraction (XRD) was used to study the crystal structure of the synthesized nanoparticles, and the diffraction positions reveal the structure. Sharp and well-defined peaks were observed in the XRD patterns of ZnO NPs, confirming the formation of a hexagonal wurtzite structure. The characteristic diffraction peaks were identified at 2 theta values: 31.7°, 34.5°, 36.1°, 47.6°, 56.7°, 62.9°, 66.4°, 67.9°, 69.1°, 72.7° & 77.1° which are attributed to the lattice planes (1 0 0), (0 0 2), (1 0 1), (1 0 2), (1 1 0), (1 0 3), (2 0 0), (1 1 2), (2 0 1). (0 0 4) & (202) respectively. According to JCPDS standard diffraction card No. 36-1451. Figure 7 shows the X-ray Diffraction XRD patterns obtained for Zinc Oxide NPs. The high-intensity and sharp diffraction peaks indicate the absence of secondary phases and a high degree of crystallinity and purity in the synthesized nano-particles [18]. The average crystallite size was estimated using the Debye–Scherer equation, and the calculation was based on the most prominent characteristic peak of the diffraction plane (101), and the average particle size is listed in Table 1.

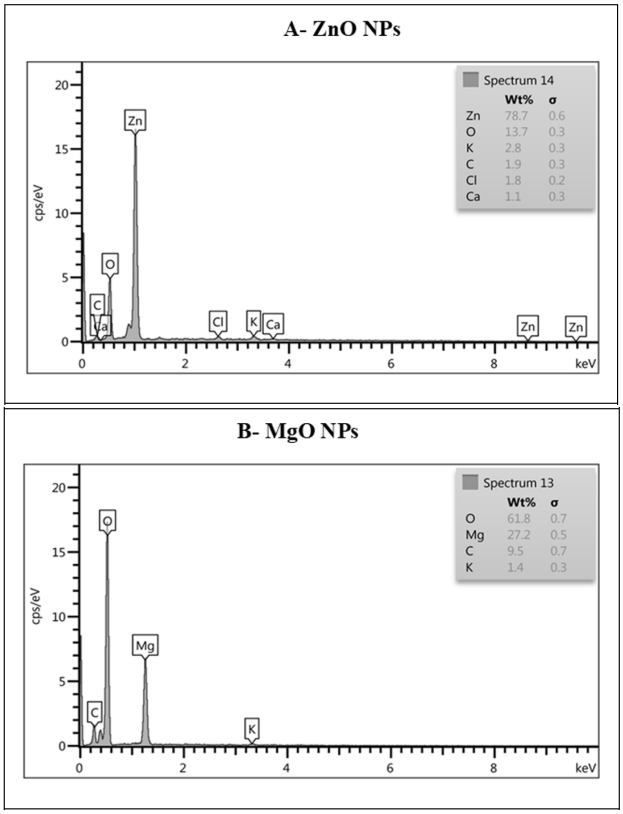

Figure 6. EDX Analysis Technology, A- ZnO nanoparticles, B- MgO nanoparticles.

Table 1. Structural information of zinc oxide nanoparticles.

Peak No:	2 θ	FWHM	D (nm)	δ	S.A*10^{21} nm^2/gm
1	31.8	0.39	0.015	4444.4	71.3
2	34.4	0.35	0.024	1736.1	44.6
3	36.3	0.14	0.019	2770.1	56.3
4	47.6	0.52	0.017	3460.2	62.9
5	56.7	0.60	14.32	4.9	0.07
6	62.9	0.66	14.44	4.8	0.1
7	66.4	0.94	8.3	0.01	0.13
8	68.1	0.79	11.9	7.1	0.09
9	69.1	0.74	13.002	5.9	0.18
10	72.6	0.61	17.1	3.4	0.06
11	77.01	0.79	12.7	6.2	0.08
			Ave.	Ave.	Ave.
			8.35	1131.19	21.44

- **Magnesium oxide nanoparticles**
  For MgO nanoparticles in Figure 7, a series of diffraction peaks at 2θ values of 36.8°, 42.8°, 62.4°, 74.0°, and 78.8° are attributed to the (111), (200), (220), (311), and (222) planes, respectively. The obtained diffraction peaks were compared with those reported in previous studies, and it was found that all the diffraction peaks are due to the pure cubic phase of MgO. In addition, the Joint Committee on Powder Diffraction Standards (JCPDS) standard card No. 89-7746 confirmed that these peaks are in agreement with the diffraction patterns [20]. Some impurity peaks were observed because of plant extracts. Moreover, the strong and sharp diffraction peaks confirm the high crystallinity of the resulting compound. The average crystallite size (full-width at half maximum, FWHM) of the MgO nanoparticles was determined from the XRD patterns using the well-known Scherrer formula, according to Table 2.

Table 2. Structural information of magnesium oxide nanoparticles.

Peak No:	2 θ	FWHM	D(nm)	δ	S.A*10^{21} nm^2/gm
1	33.4	0.47891	18.0	0.003	0.09
2	42.8	0.60384	13.5	5.5	0.12
3	62.4	0.38798	7.44	0.02	0.22
4	78.8	0.43003	7.4	0.01	0.23
			Ave.	Ave.	Ave.
			11.585	1.38	0.165

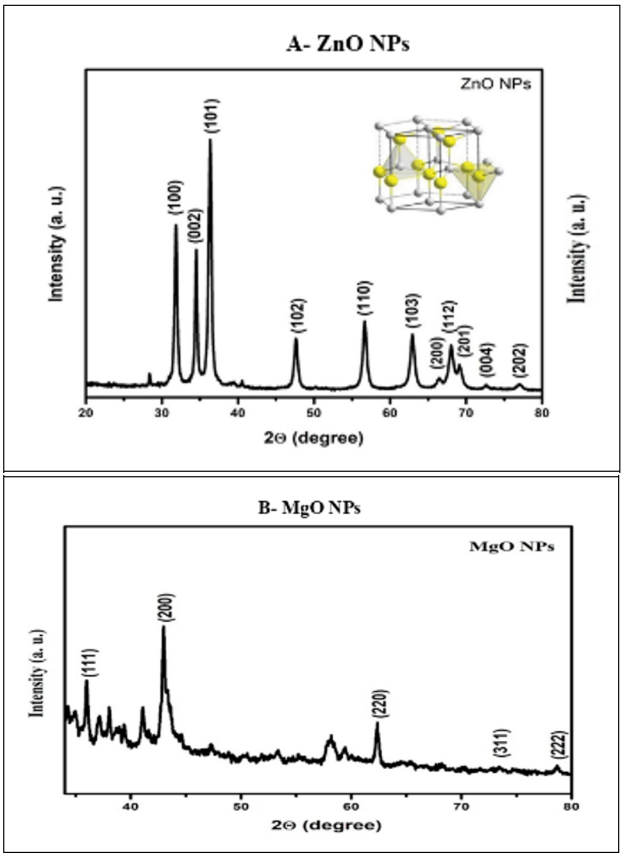

Figure 7. X-ray diffraction (XRD), A- ZnO nanoparticles, B- MgO nanoparticles.

6. CONCLUSIONS

Chamomile plant extracts were used to synthesize ZnO nanoparticles, MgO nanoparticles within the nano range. The ZnO nanoparticles had a nanosize size ranging between 55 and 70 nm, which was smaller than that of the MgO nanoparticles (60–75 nm). The crystalline nature of

the ZnO nanoparticles, which had a hexagonal structure with a wurtzite phase, was confirmed, whereas the MgO nanoparticles had a cubic face-centered (Fcc) structure.

REFERENCES

[1] L. S. Alhiti and I. H. Ali, "Photodetector fabrication and characterization of gold-cerium oxide nanoparticles for next-generation high-efficiency devices," *J. Physics: Conf. Ser.*, vol. 2974, no. 1, p. 012 033, 2025. DOI: 10.1088/1742-6596/2974/1/012033.

[2] K. Savkin et al., "Synthesis of magnesium oxide and zinc oxide powders in a glow discharge plasma at atmospheric pressure," *Ceram. Int.*, vol. 50, no. 5, pp. 8185–8197, 2024. DOI: 10.1016/j.ceramint.2023.12.150.

[3] S. P. Singh, H. Yadav, H. Chauhan, V. Hada, and K. N. Singh, "Novel approach to enhance antifungal properties via formation of wavy and sharp microstructures composed of metal oxide nanoparticles and cdots," *Sci. Reports*, vol. 15, no. 1, p. 25 483, 2025. DOI: 10.1038/s41598-025-10897-z.

[4] A. Abubakar and M. Haque, "Preparation of medicinal plants: Basic extraction and fractionation procedures for experimental purposes," *J. Pharm. Bioallied Sci.*, vol. 12, no. 1, p. 1, 2020. DOI: 10.4103/jpbs.JPBS_175_19.

[5] "Green methods for gold nanoparticle synthesis: Properties, characterization, and diverse applications," *Humanit. Nat. Sci. J.*, vol. 6, no. 2, 2025. DOI: 10.53796/hnsj63/12.

[6] S. O. Ogunyemi et al., "Green synthesis of zinc oxide nanoparticles using different plant extracts and their antibacterial activity against xanthomonas oryzae pv. oryzae," *Artif. Cells, Nanomedicine, Biotechnol.*, vol. 47, no. 1, pp. 341–352, 2019. DOI: 10.1080/21691401.2018.1557671.

[7] E. R. Essien, V. N. Atasie, A. O. Okeafor, and D. O. Nwude, "Biogenic synthesis of magnesium oxide nanoparticles using manihot esculenta (crantz) leaf extract," *Int. Nano Lett.*, vol. 10, no. 1, pp. 43–48, 2020. DOI: 10.1007/s40089-019-00290-w.

[8] A. A. Silva, A. M. F. Sousa, C. R. G. Furtado, and N. M. F. Carvalho, "Green magnesium oxide prepared by plant extracts: Synthesis, properties and applications," *Mater. Today Sustain.*, vol. 20, p. 100 203, 2022. DOI: 10.1016/j.mtsust.2022.100203.

[9] L. S. Alhiti, R. A. Jawad, R. A. Abd Alwaahed, and H. M. Sobhi, "Study of the effect of thin layer thickness on the structural properties of copper phthalocyanine (cupc) films prepared by vacuum thermal evaporation method," *Al-Kitab J. for Pure Sci.*, vol. 8, no. 01, pp. 81–91, 2024. DOI: 10.32441/kjps.08.01.p8.

[10] A. A. Q. Younis, L. S. Alhiti, G. A. Naeem, B. H. Musa, and H. R. Lateef, "Preparation of gold nanoparticles from e-waste using environmentally friendly techniques and their optical and structural study," in *Annales de Chimie. Science des Materiaux*, vol. 49, 2025, pp. 435–440. DOI: 10.18280/acsm.490411.

[11] I. H. Ali, H. O. Saheb, L. S. Alhiti, and A. A. Al-Fahham, "Spectroscopy: Types, principles and clinical uses," *Int. J. Health Med. Res.*, vol. 3, no. 7, 2024. DOI: 10.58806/ijhmr.2024.v3i07n08.

[12] M. L. Kahn, T. Cardinal, B. Bousquet, M. Monge, V. Jubera, and B. Chaudret, "Optical properties of zinc oxide nanoparticles and nanorods synthesized using an organometallic method," *ChemPhysChem*, vol. 7, no. 11, pp. 2392–2397, 2006. DOI: 10.1002/cphc.200600184.

[13] M. A. Zwijnenburg, "The effect of particle size on the optical and electronic properties of magnesium oxide nanoparticles," *Phys. Chem. Chem. Phys.*, vol. 23, no. 38, pp. 21 579–21 590, 2021. DOI: 10.1039/D1CP02683F.

[14] R. Brayner et al., "Zno nanoparticles: Synthesis, characterization, and ecotoxicological studies," *Langmuir*, vol. 26, no. 9, pp. 6522–6528, 2010. DOI: 10.1021/la100293s.

[15] A. C. Mohan and B. Renjanadevi, "Preparation of zinc oxide nanoparticles and its characterization using scanning electron microscopy (sem) and x-ray diffraction (xrd)," *Procedia Technol.*, vol. 24, pp. 761–766, 2016. DOI: 10.1016/j.protcy.2016.05.078.

[16] J. Hornak, "Synthesis, properties, and selected technical applications of magnesium oxide nanoparticles: A review," *Int. J. Mol. Sci.*, vol. 22, no. 23, p. 12 752, 2021. DOI: 10.3390/ijms222312752.

[17] K. Ramanujam and M. Sundrarajan, "Antibacterial effects of biosynthesized mgo nanoparticles using ethanolic fruit extract of emblica officinalis," *J. Photochem. Photobiol. B*, vol. 141, pp. 296–300, 2014. DOI: 10.1016/j.jphotobiol.2014.09.011.

[18] S. Fakhari, M. Jamzad, and H. Kabiri Fard, "Green synthesis of zinc oxide nanoparticles: A comparison," *Green Chem. Lett. Rev.*, vol. 12, no. 1, pp. 19–24, 2019. DOI: 10.1080/17518253.2018.1547925.

[19] K. Jhansi et al., "Biosynthesis of mgo nanoparticles using mushroom extract: Effect on peanut (arachis hypogaea l.) seed germination," *3 Biotech*, vol. 7, no. 4, p. 263, 2017. DOI: 10.1007/s13205-017-0894-3.

[20] N. Rani, S. Chahal, A. S. Chauhan, P. Kumar, R. Shukla, and S. K. Singh, "X-ray analysis of mgo nanoparticles by modified scherer's williamson-hall and size-strain method," *Mater. Today: Proc.*, vol. 12, pp. 543–548, 2019. DOI: 10.1016/j.matpr.2019.03.096.